Supporting Information

Detection of Small-Sized DNA Fragment in a Glassy Nanopore by Utilization of CRISPR-Cas12a Platform as a Converter System

Shumin Zhang[a], Minyi Liu[a], Haofa Cui[a], Muhammad Asad Ziaee[a], Rongwei Sun[a], Liting Chen[a], Daqi Chen[a,*], Denis Garoli[b,c*], and Jiahai Wang[a,*]

[a]*School of Mechanical and Electrical Engineering, School of Chemistry and Chemical Engineering, Guangzhou University, Guangzhou, 510006, China*

[b]*Istituto Italiano di Tecnologia, Via Morego 30, 16136 Genova, Italy*

[c]*Liberà Università di Bolzano, Piazza Università 1, 39100 Bolzano, Italy*

E-mail: daqichen@gzhu.edu.cn; denis.garoli@iit.it; jiahaiwang@gzhu.edu.cn

Oligonucleotides

Table S1 Oligonucleotides used in this study.

Name	Sequences (5'- 3')
Biotin-DNA (long)	biotin-(T80)-CACAAATCCTAAACG
Biotin-DNA (short)	biotin-(T10)-CACAAATCCTAAACG

Tetrahedron- A	GCCTGGAGATACATGCACATTACGGCTTTCCCTATTA GAAGGTCTCAGGTGCGCGTTTCGGTAAGTAGACGGG ACCAGTTCGCC
Tetrahedron- B	CGCGCACCTGAGACCTTCTAATAGGGTTTGCGACAGT CGTTCAACTAGAATGCCCTTTGGGCTGTTCCGGGTGT GGCTCGTCGG
Tetrahedron- C	GGCCGAGGACTCCTGCTCCGCTGCGGTTTGGCGAACT GGTCCCGTCTACTTACCGTTTCCGACGAGCCACACCC GGAACAGCCC
Tetrahedron- D	GCCGTAATGTGCATGTATCTCCAGGCTTTCCGCAGCG GAGCAGGAGTCCTCGGCCTTTGGGCATTCTAGTTGAA CGACTGTCGCCGTTTAGGATTTGTG
HPV18 target	AATTTA**ACAATATGTGCTTCTACACA**GTCTCCTGTA CCT
HIV target	TATCACCTAGAACTTTA**AATGCATGGGTAAAAGTAG TA**GAAGAGAAGGCT
crRNA	UAAUUUCUACUAAGUGUAGAU**ACAAUAUGUGCUUC UACACA**
Tetrahedron- A-7	GAGCGTTAGCCACACACACAGTC
Tetrahedron- B-7	TTAGGCGAGTGTGGCAGAGGTGT
Tetrahedron- C-7	CGCCTAAACAAGTGGAGACTGTG
Tetrahedron- D-7	AACGCTCACCACTTGAACACCTCCGTTTAGGATTTGT G
Tetrahedron- A-13	ACACTACGTCAGAACAGCTTGCATCACTGGTCACCAG AGTA
Tetrahedron- B-13	ACGAGCGAGTTGATGTGATGCAAGCTGAATGCGAGG GTCCT
Tetrahedron- C-13	TCAACTCGCTCGTAACTACACTGTGCAATACTCTGGT GACC

Tetrahedron- D-13	TCTGACGTAGTGTATGCACAGTGTAGTAAGGACCCTC GCATCGTTTAGGATTTGTG
Cube-A	GGCAACGTTTAGATCCCTCGGCTTTTAGCGCCGGCCG TTTATCTCCCACACGTTTCCACG
Cube-B	GGGAAACTTTACGTGATCGGTCTTTCGTTGCCCGTGG TTTCCTAGATCTACGTTTCGGTC
Cube-C	GGACATGTTTTCGAGACAGCAGTTTGTTTCCCGACCG TTTAGCGGATTGTACTTTCTAGG
Cube-D	GGCGCTATTTCGACCTTCTGCATTTCATGTCCCCTAGT TTACTTAATGACTGTTTCGGCC
Cube-E	GGGAGATTTTCAGTCATTAAGTTTTGTACAATCCGCT TTTCGTAGATCTAGGTTTCGTGT
Cube-F	GGGATCTTTTGACCGATCACGTTTTCTGCTGTCTCGAT TTTGCAGAAGGTCGTTTGCCGA
Bucket-1	AGCGAACGTGGATTTTGTCCGACATCGGCAAGCTCCC TTTTTCGACTATT
Bucket-2	CCGATGTCGGACATTCGCTGCGCGGTTTTTTTAAGTA ATCACGTTCACGATCTTCGCCTGCTGGGTTTTGGGAG CTTG
Bucket-3	CGAAGATCGTGTTTTTCCACAGTTGATTGCCCTTCAC TTTTCCCAGCAGG
Bucket-4	AATCAACTGTGGTTTTTCTCACTGGTGATTAGAATGC TTTTGTGAAGGGC
Bucket-5	TCACCAGTGAGATAGTCACGATATTTTGCACGTCATA TTATGTCGTACCAGGTGCATGGATTTTTGCATTCTAA
Bucket-6	CCTGGTACGACATTTTTCCACGTTCGCTAATAGTCGA TTTTATCCATGCA
Bucket-lid	AACCGCGCAGCGTTTTTTTTTTATGACGTGCTTTTTTT TTATCGTGACGGTTGGTGTGGTTGGCGTGATTACTTA

Tri-prism-V1	TCCTAAAGCATGACCTTCCGAACATTCGAGGCACGTTGTACGTCCACACTTGGAACCTCATCGCACATCCGCCTGCCACGCTCTTGTTTCAAGCGCAGCCAGATT
Tri-prism-V2	TCTTCTGATCCTTAACGGCCAACATTCGAGGCACGTTGTACGTCCACACTTGGAACCTCATCGCACATCCGCCTGCCACGCTCTTTTGCTGAACTTTGGTTTGAT
Tri-prism-C1	TGTTATCTCCGACGGTACTTCGTACAACGTGCCTCGAATGTAGAGCGTGGCAGGCGGATGTGAAGCAGTTGCACCGGCATTGTC
Tri-prism-C2	GTCACTACTAATACACCTGTCGATGAGGTTCCAAGTGTGGATAGCTAGGTAAGACCGCATCTC
Tri-prism-R1	AATGCCGGTGCAACTGCTACCAGGTGTATTAGTAGTGACGAC
Tri-prism-R2	ATGCGGTCTTACCTAGCTCCAGTACCGTCGGAGATAACAGAG

Table S2 Detailed compositions of NEBuffer 2.1, NEBuffer 2.1 with removal of BSA, NEBuffer 2.1 with BSA replaced by DTT and IDT buffer

Buffer	**Compositions**
NEBuffer 2.1 (1X)	50 mM NaCl 10 mM Tris-HCl 10 mM $MgCl_2$ 100 μg/ml BSA pH 7.9@25°C
NEBuffer 2.1 with removal of BSA	50mM NaCl

(1X)	10mM Tris-HCl 10mM $MgCl_2$ PH 7.9@25°C
NEBuffer 2.1 with BSA replaced by DTT (1X)	50 mM NaCl 10 mM Tris-HCl 10 mM $MgCl_2$ 1mM DTT pH 7.9@25°C
IDT buffer (1X)	100mM NaCl 5mM $MgCl_2$ 20mM HEPES 0.1 mM EDTA pH 6.5@25°C

Characterization of DNA tetrahedron

The self-assembled DNA tetrahedron was analyzed by 12% native PAGE. DNA tetrahedron composed with four strands (lane 7) showed the lowest mobility compared with the hybridization products of three strands (lanes 5 - 6), double-stranded DNA (dsDNA) (lanes 3 - 4), and the single strand DNA (ssDNA) (lanes 1 - 2) (Fig. S1), indicating the formation of DNA tetrahedron with the increased mass and spatial complexity. In lanes 5 - 7, besides the products we expected, there are some larger structures due to the formation of multimers. But fortunately, the existence of these big structures will not affect our experiment.

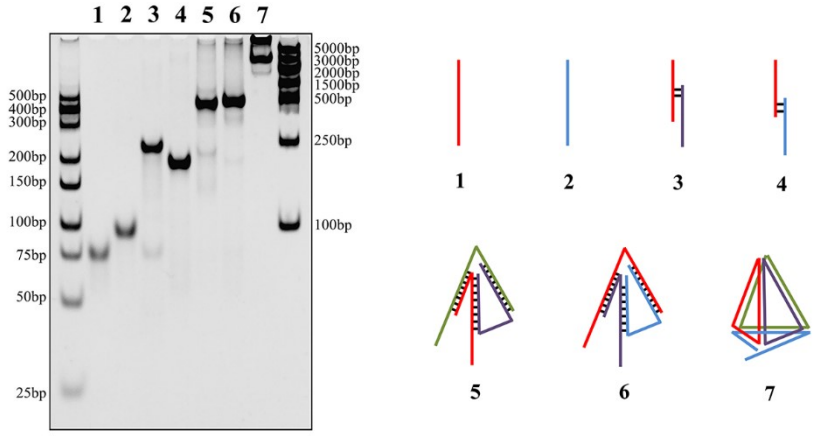

Fig. S1 Native-PAGE (12%) analysis of the mixtures of all four required fragments for formation of DNA tetrahedron (10 μM) (lane 7), the hybridization products of single (lanes 1 -2), two (lanes 3 -4) or three (lanes 5 -6) strands (10 μM for each product).

DNA nanostructure optimization

The shape and size of DNA nanostructure play critical roles in generating detection signals in glass nanopore. Due to the extensibility of our conversion method, different DNA nanostructures are able to incorporate to enlarge signal of small-sized DNA fragment. We tested the signals of different nanostructures and the signal of different DNA nanostructures were shown in Fig.S2 and the sequences were demonstrated in Table S1. All the structures (tetrahedron, cube, bucket and triangular prism) can produce detectable signals when they pass through the glassy nanopore. However, synthesis of DNA bucket and triangular prism is too complicated and the signal reproducibility of these two nanostructures were not very good. Signal of DNA cube owned the highest signal-to-noise ratio and good reproducibility. However, the temperature stability of DNA cube was poor. After incubated with CRISPR-Cas system

at 37 ℃, the event rate of DNA cube dropped evidently (shown in Fig. S3) and not suitable for this application. Therefore, we chose DNA tetrahedron as signal amplification molecule for its simplicity of synthesis, good and reproducible signal and excellent temperature stability.

As for DNA tetrahedrons with different sizes, we referred to several works. There are DNA tetrahedrons that the lengths of their sides were 7nt,13nt and 26nt, respectively (sequences were also shown in Table S1). In order to reduce the pore size requirement of glassy nanopores, making it easier to fabricate and with better reproducibility, we choose the largest tetrahedron structure (26nt) in this work. However, we did not use DNA tetrahedron with a side length of more than 26nt, because this will cause the DNA oligonucleotides for synthesis of tetrahedron to exceed 100nt, leading to a sharp increase in the cost of synthesizing these DNA oligonucleotides. This additional cost increase is undesirable in practical application. Therefore, we finally chose the nucleic acid tetrahedron with a side length of 26nt.

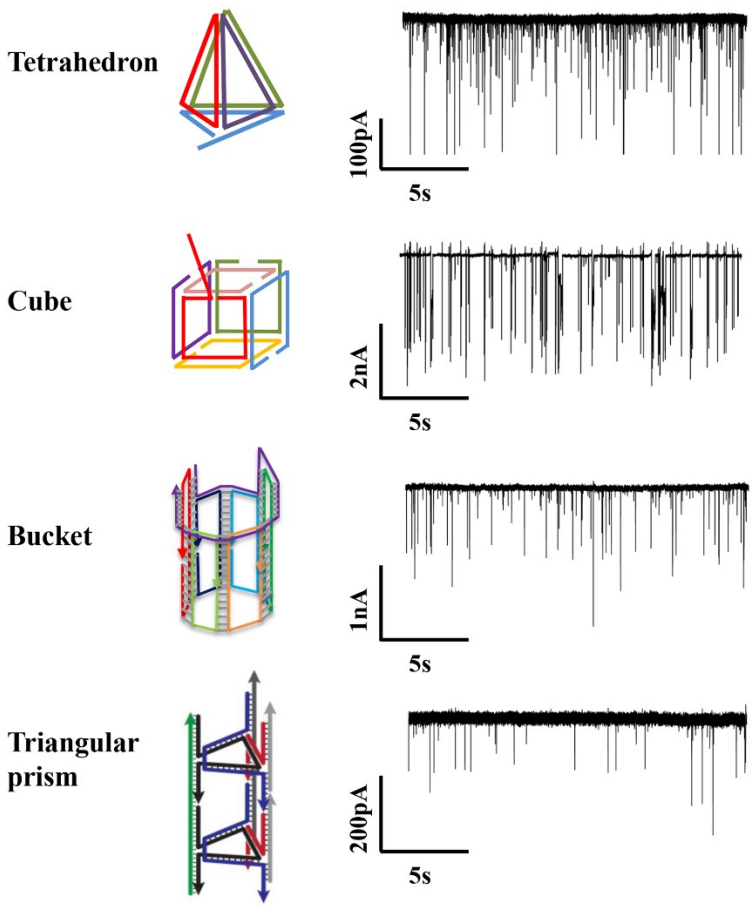

Fig. S2 Signal of different DNA nanostructures.

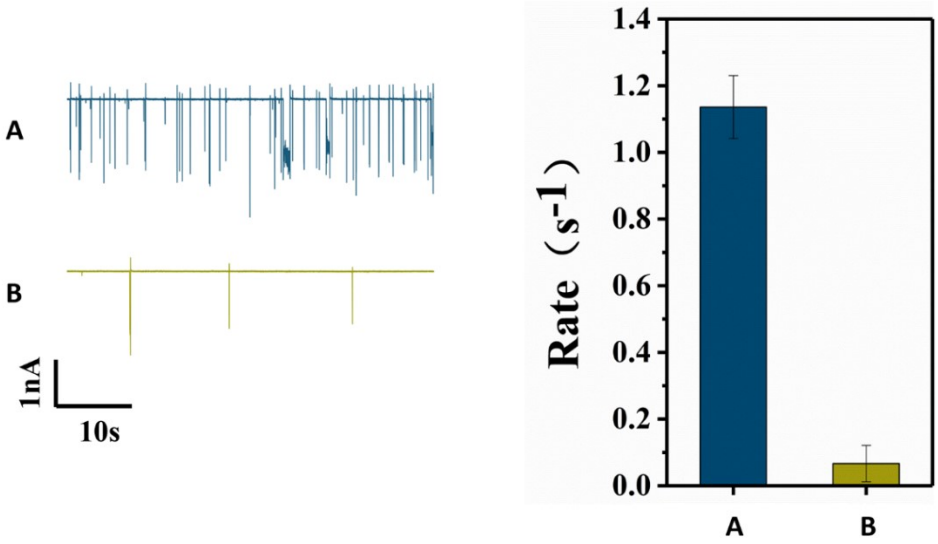

Fig. S3 Signal of DNA cube before and after incubated in 37℃ for an hour. (a) before;

(b) after.

Reproducibility of the translocation signals of DNA tetrahedron

The translocation signals of DNA tetrahedron through nanopores fabricated with different parameters were shown in Fig. S4. The concentrations of DNA tetrahedrons were all 50 nM. Although the difference of pore size is very large, with the pore size ranging from 25 to over 65 nm, but the event rate maintains stable in a wide range, suggesting that using tetrahedron as a signal transducer is good way to maintain good reproducibility when the pore size of the glass nanopores fluctuates between batches.

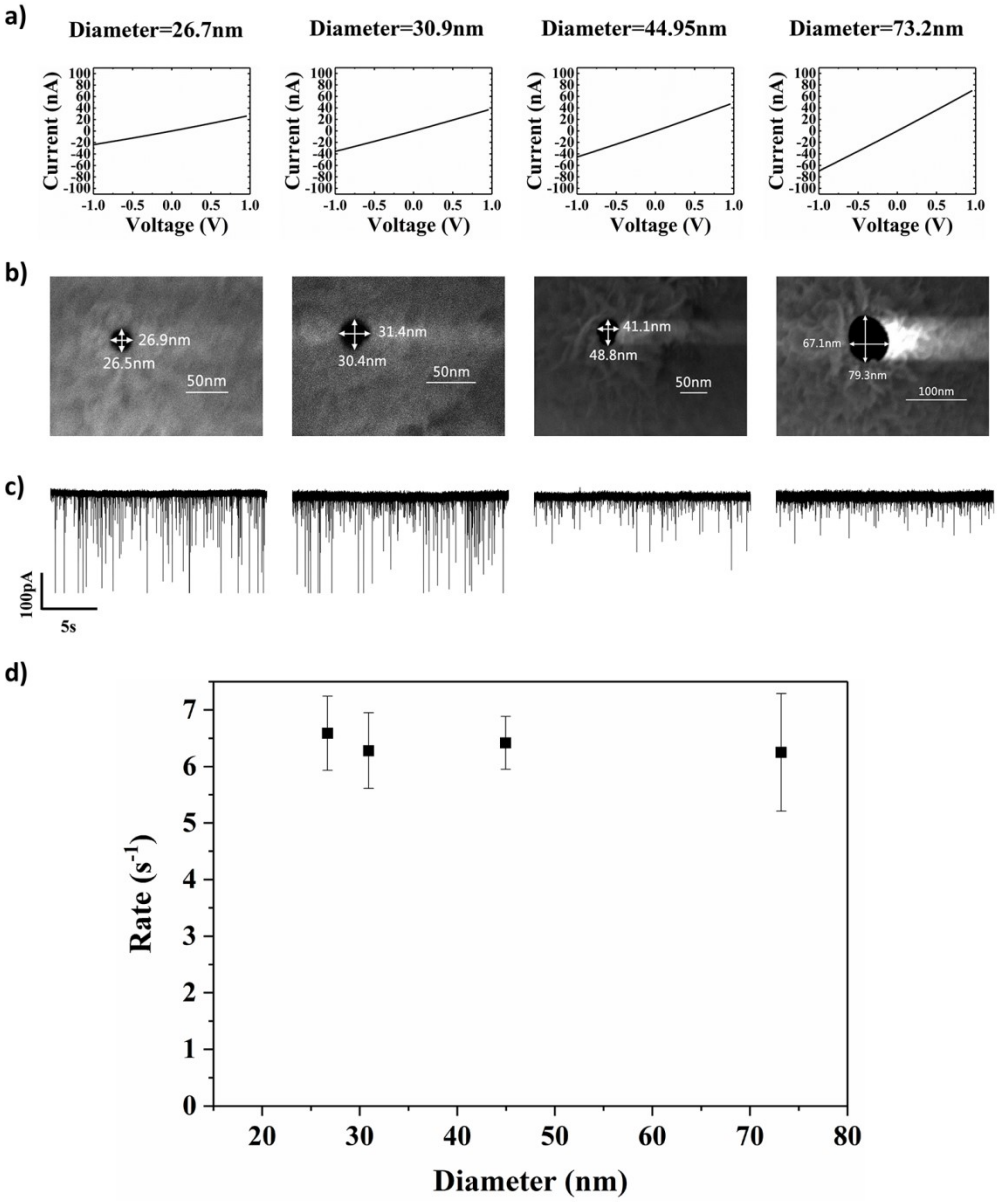

Fig. S4 Signal repeatability experiment of DNA tetrahedron transducer. (a) I-V curves

of glass nanopores fabricated with different parameter, showing different slope. (b) SEM image of the glassy nanopore. (c) Translocation recording of the DNA tetrahedron with different pore size of glassy nanopores. Although the amplitude of the current pulse becomes lower with the increase of the pore size, there is no significant change in the event rate within a wide range of pore size. (d)The event rate of the sensor with different nanopore diameter, ranging from 25 to 75 nm.

Optimization of the amount magnetic bead

The amount of magnetic bead was optimized from 0 μL to 35 μL so that it could efficiently bind the biotin-DNA, which fetch the tetrahedron from the solution onto the surface of magnetic particle. By increasing the amount of magnetic up to 25 μL, the event rate decreased correspondingly. After the amount of magnetic bead exceeded 25 μL, the event rate decreased to 0 s^{-1}. To ensure a blank baseline, 30 ul magnetic bead was selected in this work.

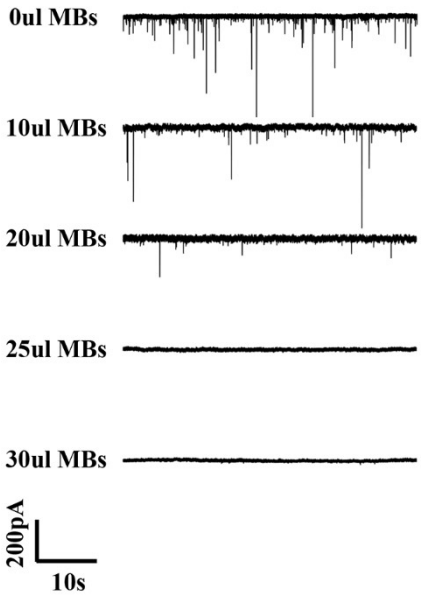

Fig. S5 The event rate when different amount of magnetic bead was used.

Optimization of the bias voltage

We also tried different bias voltages in the experiment and the result was shown in Fig. S6. Higher voltages result in higher signal rate. However, using high bias voltage was easy to cause the blockage of the glassy nanopore. Finally, a 400mV bias voltage was applied in this experiment.

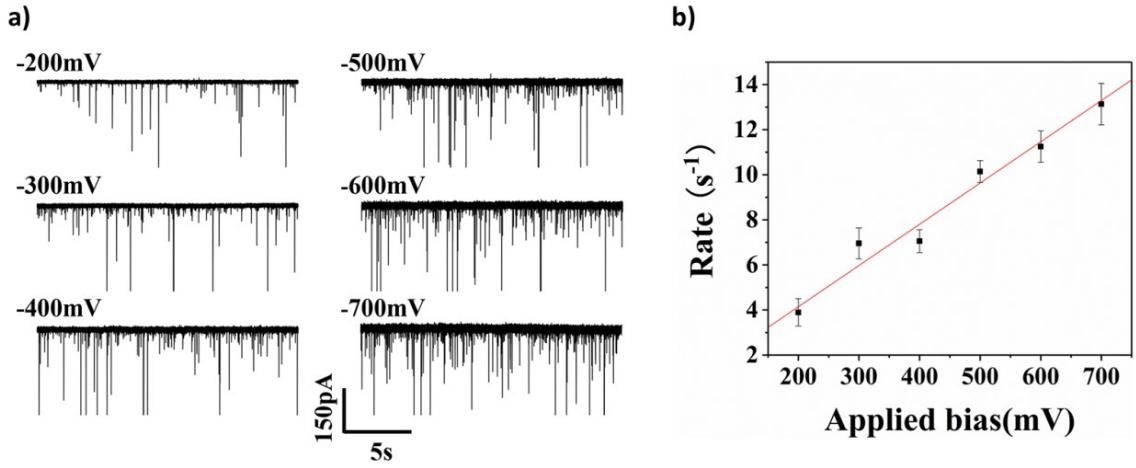

Fig. S6 Detection of different applied bias of DNA tetrahedron. (a) Translocation recording of the sensor with 50 nM DNA tetrahedron at different applied bias. (b) event rate versus applied bias of 50 nM DNA tetrahedron.

Calibrating the sensor with known concentration of DNA tetrahedron

We calibrated our sensor with known concentration of DNA tetrahedron to find out the event rate of different concentration of DNA tetrahedral. As shown in Fig. S7, with the increase of tetrahedral concentration, the event rate increases linearly. In our experiment, if all DNA tetrahedron was released into the solution from the magnetic bead, the final concentration would be 33.3 nM. According to Fig. S7, the event rate was about 5 s^{-1} when the concentration of DNA tetrahedron was about 33.3 nM.

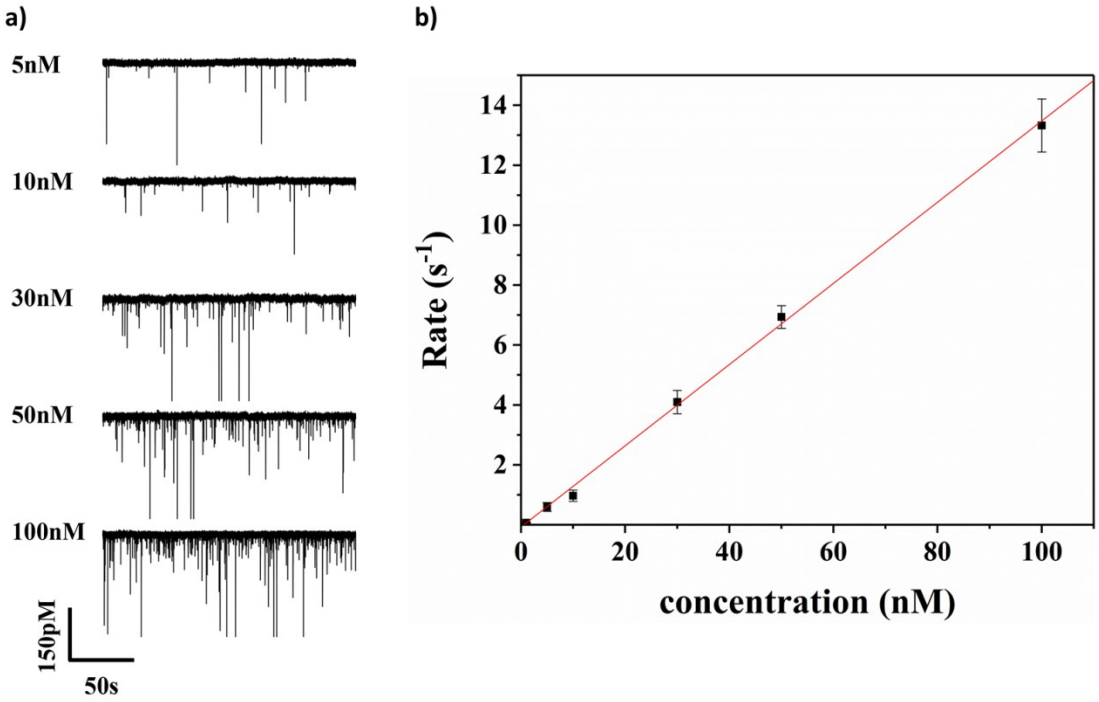

Fig. S7 Detection of different concentration of DNA tetrahedron. (a) Translocation recording of the sensor with different concentration of DNA tetrahedron under 400 mV bias. (b) Calibration curve of the sensor with DNA tetrahedron ranging from 1 nM to 100 nM.